

Analyst

Accepted Manuscript



This is an *Accepted Manuscript*, which has been through the Royal Society of Chemistry peer review process and has been accepted for publication.

Accepted Manuscripts are published online shortly after acceptance, before technical editing, formatting and proof reading. Using this free service, authors can make their results available to the community, in citable form, before we publish the edited article. We will replace this *Accepted Manuscript* with the edited and formatted *Advance Article* as soon as it is available.

You can find more information about *Accepted Manuscripts* in the [Information for Authors](#).

Please note that technical editing may introduce minor changes to the text and/or graphics, which may alter content. The journal's standard [Terms & Conditions](#) and the [Ethical guidelines](#) still apply. In no event shall the Royal Society of Chemistry be held responsible for any errors or omissions in this *Accepted Manuscript* or any consequences arising from the use of any information it contains.

An ultra-high throughput spiral microfluidic biochip for the enrichment of circulating tumor cells

Majid Ebrahimi Warkiani^{1#}, Bee Luan Khoo^{2,3#}, Daniel Shao-Weng Tan⁴, Ali Asgar S. Bhagat⁵, Wan-Teck Lim⁴, Yoon Sim Yap⁴, Soo Chin Lee⁶, Ross A. Soo⁶, Jongyoon Han^{1,7*}, Chwee Teck Lim^{1,2,3,5*}

¹BioSystems and Micromechanics (BioSyM) IRG, Singapore-MIT Alliance for Research and Technology (SMART) Centre, Singapore

²Mechanobiology Institute, National University of Singapore, Singapore

³Department of Biomedical Engineering, National University of Singapore, Singapore

⁴Department of Medical Oncology, National Cancer Centre Singapore, Singapore

⁵Clearbridge BioMedics Pte Ltd, Singapore

⁶Department of Hematology-Oncology, National University Hospital, Singapore

⁷Department of Electrical Engineering and Computer Science, Department of Biological Engineering, Massachusetts Institute of Technology, Cambridge, Massachusetts, USA

These authors contributed equally to this paper.

*Contact:

Jongyoon Han ([jyhan@mit.edu](mailto: jyhan@mit.edu))
Room 36-841, Research Laboratory of Electronics,
Massachusetts Institute of Technology
77 Massachusetts Avenue, Cambridge, MA 02139, USA

Chwee Teck Lim ([ctlim@nus.edu.sg](mailto: ctim@nus.edu.sg))
Department of Bioengineering, National University of Singapore,
9 Engineering Drive 1, Singapore 117576, Singapore

ABSTRACT

Detection and characterization of rare circulating tumor cells (CTCs) from blood of cancer patients can potentially provide critical insights into tumor biology and hold great promise for cancer management. The ability to collect a large number of viable CTCs for various downstream assays such as quantitative measurements of specific biomarkers or targeted somatic mutation analysis is increasingly important in medical oncology. Here, we present a simple yet reliable microfluidic device for the ultra-high throughput, label-free, size-based isolation of CTCs from clinically relevant blood volumes. The fast processing time of the technique (7.5 mL blood in less than 10 mins) and ability to collect more CTCs from larger blood volume lends itself to a broad range of potential genomic and transcriptomic applications. A critical advantage of this protocol is the ability to return all fractions of blood (i.e., plasma (centrifugation), CTCs and white blood cells (WBCs) (size-based sorting)) that can be utilized for diverse biomarker studies or time-sensitive molecular assays such as qRT-PCR. The clinical use of this biochip was demonstrated by detecting CTCs from 100% (10/10) of blood samples collected from patients with advanced stage metastatic breast and lung cancer. CTC recovery rate ranged from 20-135 CTCs/mL and obtained under high purity (1 CTC for every 30-100 white blood cells detected, ~ 4 log depletion of WBCs). They were identified with immunofluorescence assays (Pan-cytokeratin+/CD45-) and molecular probes such as *HER2/neu*.

KEYWORDS: Circulating tumor cells (CTCs); Microfluidics; Cancer; Cell separation; Blood

INTRODUCTION

Circulating tumor cells (CTCs), cancer cells of solid tumor origin that shed into the blood stream from either primary or secondary tumors of patients, directly contribute to the haematogenous metastatic spread and subsequent growth of tumor cells at distant sites within the body.^{1, 2} The isolation and recovery of these CTCs are very challenging primarily due to their rarity in peripheral blood and also their heterogeneity.³ Nevertheless, enrichment of CTCs can help clinicians better understand the biology of metastasis and disease progression as well as contribute to cancer management by potentially serving as a powerful clinical prognostic tool and non-invasive analysis of tumor genotypes for the therapeutic management of cancer-related diseases.^{3, 4} However, conventional clinical approaches for isolation of CTCs from peripheral blood, including flow cytometry,⁵ gradient centrifugation,⁶ and fluorescence and magnetic-activated cell sorting^{7, 8} are often based on antigen recognition techniques, which are expensive and limited in yield and purity. Most techniques require long processing time, resulting in low cell viability of the enriched CTCs. They also do not allow complete fractionation and preservation of plasma, white blood cells (WBCs) and CTCs. A reliable method for rapid, efficient and effective enrichment of CTCs will therefore be pivotal for deepening our understanding of the metastatic process and contribute to the field of clinical oncology.

Microfluidics is one of the most rapidly developing technologies for innovation in cancer research. The application of microfluidic systems for separation of CTCs provides unprecedented opportunities for efficient enrichments of these rare cells from blood, allowing detailed molecular characterization of them at the single-cell level.⁹ While several microfluidic devices have been reported for CTCs isolation using epithelial cell surface antigens such as EpCAM (epithelial cell adhesion molecule),^{10, 11} these platforms/techniques rely on mediating the interaction of target CTCs with anti EpCAM-coated features including

1
2
3 micropillars¹⁰ or nanoporous surfaces¹² under precisely controlled laminar conditions with
4
5 reliable efficiency. However, some tumor cells express low or no EpCAM (e.g., for cells that
6
7 undergo epithelial-mesenchymal transition (EMT)), resulting in incomplete retrieval of
8
9 isolated CTCs.^{1, 13} In addition, the immunomagnetic isolation approaches involve chemical
10
11 and mechanical manipulation of the cells rendering them non-viable or challenging for
12
13 culture as well as downstream molecular analysis.^{14, 15} To date, a number of microfluidic
14
15 devices that employ dielectrophoretic forces have also been developed for isolation of cancer
16
17 cells based on differences in responses of cells to the electric field.^{14, 16, 17} Although this
18
19 allows for label-free cell sorting without relying on immunochemistry, this technique is
20
21 limited due to the subtle dielectric differences between CTCs and blood cells thereby
22
23 affecting the throughput and purity and the high electric fields that can potentially cause gene
24
25 expression (phenotypic) changes.¹⁸ To overcome the above limitations, cell size and
26
27 deformability have been exploited in order to isolate CTCs from blood. Most CTCs are
28
29 believed to be larger than the other blood components (< 20 μ m) (RBCs, peripheral WBCs
30
31 and platelets),^{19, 20} including tumor cells obtained from small cell lung cancer patients.²¹ This
32
33 obviates the need for any prior knowledge of target cells' biochemical characteristics, while
34
35 enabling collection of putative CTCs regardless of their EpCAM expression. The most
36
37 popular size/deformability based CTC isolation methods rely on using either track-etched
38
39 membranes or microfabricated filters.^{22, 23} These techniques are limited by the volume of
40
41 blood that can be processed due to issues arising from filter clogging, low recovery and low
42
43 cell viability due to cell damage caused by high shear incurred as the cells are made to pass
44
45 through the filter pores.
46
47
48
49
50

51
52 Hydrodynamic filtration systems for size-based separation in the microfluidic devices can
53
54 overcome the shortcomings of the current approaches including clogging, low recovery and
55
56 cell viability issues.^{24, 25} The controlled laminar flow within microfluidic channels can be
57
58
59
60

1
2
3 manipulated to generate size-dependent cell trajectories for high resolution CTC enrichment.
4
5 Previously, we report a novel microfluidic platform for blood fractionation (i.e., named as
6
7 “*Dean Flow Fractionation*”) and applied it successfully for CTCs isolation from whole
8
9 blood.^{25, 26} We have shown the integrated spiral biochip is capable of processing blood with
10
11 hematocrit of 20-25%, thus allowing process and enrichment of rare cells with ~3 mL/hr
12
13 speed. Herein, we report the development of a simple yet reliable multiplexed spiral biochip
14
15 for ultra-high throughput isolation, label-free isolation of CTCs to address the challenges of
16
17 the next generation CTC enrichment platform such as *high sensitivity* (near 100% detection
18
19 rate), *high purity* (~750 WBCs/mL), *high throughput* (7.5 mL in less than 10 mins), *label-*
20
21 *free* enrichment, *simplicity* and *ease of operation*. In contrast to the previous version, this
22
23 device can work with a minimum of two syringe pumps instead of three (i.e., making
24
25 automation easier) and can process larger volume of blood samples in shorter time with
26
27 relatively higher sensitivity and purity. Processing larger volume of blood samples can boost
28
29 the number of enriched CTCs for multiple downstream assays such as Immunofluorescent
30
31 staining, qRT-PCR, fluorescence in situ hybridization (FISH) and also time-sensitive
32
33 molecular tests such as RNA-sequencing. The clinical use of this biochip was demonstrated
34
35 by the isolation of CTCs from 100% (10/10) of blood samples collected from patients with
36
37 advanced stage metastatic breast and lung cancer. Retrieved cells are unlabelled and hence
38
39 more viable for propagation, drug development and other downstream analysis. This design is
40
41 extremely ideal for development of a low-cost and automated CTC detection and retrieval
42
43 device for cancer diagnosis and prognosis.
44
45
46
47
48
49
50

51 MATERIAL AND METHODS

52 Device fabrication

1
2
3 SU-8 silicon molds were fabricated using standard lithography techniques.^{27, 28} The patterned
4
5 silicon wafer was silanized with trichloro (1H, 1H, 2H, 2H-perfluorooctyl) silane (Sigma
6
7 Aldrich, USA) to render the surface hydrophobic. PDMS prepolymer was prepared by mixing
8
9 the PDMS at a standard 1:10 ratio (Sylgard 184, Dow Corning, USA) and degassing in a
10
11 vacuum chamber. To produce the single layer spiral biochip, PDMS prepolymer was poured
12
13 onto the SU-8 mold and cured 80 °C for 1-2 h inside a conventional oven. The PDMS was
14
15 then cut from the mold, and four fluidic access holes (two-inlets and two-outlets) were
16
17 punched. In order to obtain the multiplexed device, three spiral biochips were bonded
18
19 together using oxygen plasma and manual alignments. The final device obtained by bonding
20
21 the whole assembly onto a microscopic glass slide using an air plasma machine.
22
23
24
25
26

27 **Cell culture and sample preparation**

28
29 Two commercially available human cancer cell lines, namely breast adenocarcinoma (MCF-
30
31 7) and bladder (T24) were first used to mimic CTC separation. The MCF-7 cells (HTB-
32
33 22TM, ATCC, USA) and T24 cells (HTB-4 ATCC, USA) were cultured in high-glucose
34
35 Dulbecco's modified Eagle's medium (DMEM) (Invitrogen, USA) supplemented with 10%
36
37 fetal bovine serum (FBS) (Invitrogen, USA) together with 1% penicillin-streptomycin
38
39 (Invitrogen, USA). The culture was maintained at 37 °C in a humidified atmosphere
40
41 containing 5% (v/v) CO₂ till 80% confluence. Cells were cultured in sterile 6-well plates (BD
42
43 Bioscience, USA) and sub-cultivated (1:3) two times a week with media replaced every 48 h.
44
45 Sub-confluent monolayers were dissociated using 0.01% trypsin and 5.3mM EDTA solution
46
47 (Lonza, Switzerland). For the control and recovery experiments, the cancer cells were diluted
48
49 in buffer containing 1x phosphate buffered saline (PBS), 2 mM ethylenediaminetetraacetic
50
51 acid (EDTA) supplemented with 0.5% bovine serum albumin (BSA) (Miltenyi Biotec,
52
53 Germany) to prevent non-specific adsorption to the tubing and microchannel walls. For all
54
55
56
57
58
59
60

1
2
3 experiments unless otherwise mentioned, whole blood obtained from healthy donors was
4 lysed using red blood cell (RBC) lysis buffer (Bioscience, USA) for 5 mins at room
5 temperature under continuous gentle mixing. The lysed RBCs were removed by
6 centrifugation at 1000×g for 5 mins and nucleated cell fraction were re-suspended in
7 phosphate buffer saline (PBS) buffer accordingly with PBS buffer. The process of RBC lysis
8 removes blood contaminants and hence reduces overall cell concentration. Therefore,
9 nucleated cells can be resuspended in a smaller volume of buffer, speeding up the process of
10 size-based sorting by microfluidic device.
11
12
13
14
15
16
17
18
19
20

21 22 **Immunofluorescence staining and Fluorescent Automated Cytometry System** 23 **(FACS) analysis**

24
25 Results from experiments conducted to determine the cell loss incurred by lysis were
26 analyzed by performing flow cytometry analysis using a BD Accuri C6 flow cytometer (BD
27 Biosciences, USA) on the lysed and whole blood spiked samples. Samples were spiked with
28 100K T24 cells pre-stained with fluorescein isothiocyanate (FITC) conjugated pan-
29 cytokeratin (CK) antibody (1:100, Miltenyi Biotec Asia Pacific, Singapore). Outlet samples
30 were concentrated to 1 mL and processed for quantification of pan-CK⁺ cells. For
31 quantification of cell counts, Immunofluorescence (IF) staining was carried out to allow
32 visualization and differentiation of the various cell types. The outlet samples were fixed with
33 4% paraformaldehyde (PFA) (Sigma, USA) for 10 mins in room temperature, permeabilized
34 with 0.1% Triton X-100 in PBS (Sigma, USA). Permeabilized cells were treated with an
35 antibody cocktail (pan-CK antibody, APC conjugated CD45 antibody (1:100, Miltenyi Biotec
36 Asia Pacific, Singapore) and Hoechst dye in PBS buffer for 30 mins on ice. During flow
37 cytometry analysis, the cells were gated based on the forward and side scatters as well as the
38 fluorescence intensity.
39
40
41
42
43
44
45
46
47
48
49
50
51
52
53
54
55
56
57
58
59
60

Viability culture experiments

A known concentration of T24 cells were spiked into whole blood before lysis. T24 cell counts (before and after lysis) were compared by enumeration of recovered T24-spiked blood after their respective treatment. Recovered cells were seeded onto 2D substrates under optimal growth conditions and bright field images were obtained after 5 mins from seeding.

DNA Fluorescence in-situ hybridization (FISH)

Samples were obtained from patients with HER2+ tumor status. The tumors were extracted via biopsy in the diagnostic stage (pre-treatment) and analysed for gene amplification via PCR in the hospital (not shown). Cells were spun onto slides using a Cytospin centrifuge (Thermo Scientific, USA) at 600 rpm for 6 mins. Slides were fixed in 4% PFA at room temperature for 10 mins and dehydrated via ethanol series (80%, 90%, and 100%). For DNA FISH, slides were treated with RNase (4 mg/mL) (Sigma, USA) for 40 mins at 37 °C, washed with 1x PBS/0.2% Tween 20 (Sigma, USA) thrice and denatured with 70% formamide/2x SSC for 10 mins at 80 °C. They were then quench dehydrated again via ice-cold ethanol series. HER2 probes were directly applied to slides maintained at 42 °C. Hybridization was continued at 42 °C under dark and humid conditions overnight. Slides were washed with 50% formamide/ 2x SSC and 2x SSC at 45 °C under shaking, counterstained with 4', 6-diamidino-2-phenylindole (DAPI) counterstain and sealed with 50×50 mm² coverslip (Fisher Scientific, USA).

Clinical samples

Human whole blood samples were obtained from healthy donors and 10 patients with either metastatic lung or breast cancer. This study was approved by our local ethics committee according to a protocol permitted by the Institutional Review Board (IRB). A total of 5 blood

1
2
3 samples from healthy donors were used as controls and 10 samples from lung and breast
4
5 cancer patients were processed for CTC enumeration. Blood samples were collected in
6
7 vacutainer tubes (Becton-Dickinson, Franklin Lakes, NJ, USA) containing EDTA
8
9 anticoagulant and were processed within 2-4 h to prevent blood coagulation. For all the
10
11 samples, 7.5 mL of whole blood was lysed initially using RBC lysis buffer and re-suspended
12
13 in PBS prior to processing on biochip. 7.5 mL of blood is concentrated to 3.75 mL for
14
15 processing, reducing processing time. Samples are processed at an input velocity of 350
16
17 $\mu\text{l}/\text{min}$.
18
19

20 21 22 **RESULTS AND DISCUSSION**

23 24 **Working Principle**

25
26
27
28 Figure 1A schematically illustrates the principle of hydrodynamic separation in spiral
29
30 microfluidic channels. In the spiral microchannels with rectangular cross-section, the
31
32 influence of centrifugal forces acting in radial direction results in the formation of two
33
34 symmetrical counter-rotating vortices across the channel cross-section, also known as Dean
35
36 vortices. Under Poiseuille flow condition, naturally buoyant particles of varying sizes
37
38 equilibrate at different positions along the microchannel cross-section under the influence of
39
40 inertial lift and Dean drag forces.²⁴ By confining the cells at the inlet to one region of the
41
42 channel cross-section, we can effectively fractionate the cells by equilibrating the CTCs near
43
44 the microchannel inner wall while driving the smaller hematologic cells (platelets and WBCs)
45
46 to the microchannel outer wall, allowing an efficient separation at the outlet.²⁹ The spiral
47
48 biochip enriches the CTCs population by a significant 10^4 -fold from a red blood cells (RBCs)
49
50 depleted nucleated cell fraction. It consists of two-inlets and two-outlets to enrich the larger
51
52 CTCs at the outlet. The collected CTCs can then be analyzed by suitable downstream
53
54
55
56
57
58
59
60

1
2
3 techniques such as immunostaining, qRT-PCR and FISH or can be employed for culturing
4
5 and single-cell analysis (Figure 1B).
6
7

8 9 **Spiral biochip operating parameter optimization**

10
11 The challenge for clinical use of CTCs is to develop an unbiased, high throughput and
12
13 reliable assay to enrich viable CTCs from peripheral blood in a reasonable period of time.
14
15 High speed frame capture (6,400 frames per second) of CTC isolation via the spiral device is
16
17 illustrated in Figure 2A. For all the experiments, high-speed imaging was performed to
18
19 monitor position of CTCs and WBCs near the outlet region (See movie S1&S2 in
20
21 Supplementary Information). 99.9% of WBCs and residual RBCs undergo a complete Dean
22
23 Cycle migration and exit from the waste outlet while CTCs that were focused near the inner
24
25 wall during the lateral migration can be collected from the CTC outlet. To reduce the amount
26
27 of cellular components flowing in the spiral biochip, we employed a conventional RBC lysis
28
29 technique (using ammonium chloride solution) in order to process larger volume of clinical
30
31 samples. While WBCs constitute just 1% of total blood volume fraction, it is still challenging
32
33 to efficiently separate minute quantities of CTCs from them. Extensive characterization of the
34
35 proposed methodology was carried out to study the depletion capability of WBCs in the spiral
36
37 biochip. To demonstrate the impact of input sample cell concentration on the device
38
39 performance and final purity, we carried out the processing of blood under different nucleated
40
41 cell concentrations. Initial 7.5 mL whole blood collected from healthy donors had the RBCs
42
43 lysed and the nucleated cell fraction was then spun down and resuspended back to 7.5 mL (1x
44
45 concentration), 3.75 mL (2x concentration) and 2.5 mL (3x concentration), respectively.
46
47 Figure 2B shows the total cells count collected from the CTC outlet at different sample
48
49 concentrations in 5 mins. A linear incremental trend in the total cell count is observed
50
51 suggesting the effect of initial WBCs concentration on the final purity. Since the total number
52
53 of WBCs varied from one patient to another and with cancer type/stage,³⁰ we decided to use
54
55
56
57
58
59
60

1
2
3 2x concentration ($\sim 14 \times 10^6$ WBCs) as optimal for future tests and clinical validation. This
4 translates to a total processing time of around 10 mins for 7.5 mL blood sample using a
5 multiplexed device with three stacked spiral biochips (see Fig. 1).
6
7

8
9
10 Next, to demonstrate robustness and repeatability, a pure population of leukocytes was
11 processed through the biochip at 2x concentration continuously. Enriched samples containing
12 the contaminating WBCs were collected from the CTC outlet for a period of 5 mins, each
13 collection taken from different time intervals (0-5, 5-10 and 10-15 mins) from the start of
14 processing. The WBC count collected at the different time point is fairly uniform with
15 approximately 900 to 1,200 cells collected under optimal flow conditions (see Fig. 2C).
16
17
18 Microscopic analysis of the collected WBCs (data not shown) revealed that this sub-
19 population were in order of CTCs in terms of size (i.e., ~ 12 - $15 \mu\text{m}$), and can be easily
20 differentiated using immunofluorescence staining and molecular approaches. Starting with a
21 initial concentration of $\sim 7 \times 10^6$ nucleated cells, the spiral biochip depleted $\sim 99.99\%$ of the
22 WBCs providing a purer CTC fraction at the outlet. This is particularly important for many
23 downstream molecular assays where the contaminating materials from WBCs can
24 significantly lower the signal to noise leading to inaccurate diagnosis.
25
26
27
28
29
30
31
32
33
34
35
36
37
38
39
40

41 **Effect of RBC lysis on separation efficiency and cell viability**

42
43 Chemical lysis of whole blood using ammonium chloride has been employed extensively for
44 depletion of contaminated RBCs in various applications such as transcriptome analysis of
45 WBCs in various human diseases. While some people reported that RBC lysis can lead to
46 compounded loss of cells,³⁰ we have shown here depletion of RBCs did not compromise the
47 recovery and isolation of cancer cells significantly (Fig. 3A). Exposure to the lysis buffer also
48 did not alter the morphology and size of the cells (Fig. 3B).
49
50
51
52
53
54
55
56
57
58
59
60

1
2
3 We also compared the performance of our previous integrated biochip²⁶ with the new
4 multiplexed spiral one for CTC isolation. In the previous integrated biochip, whole blood was
5 processed (100 $\mu\text{l}/\text{min}$) with the two-biochip cascaded spiral device and progressively diluted
6 with a sheath flow (750 $\mu\text{l}/\text{min}$) running through the device. 7.5 mL of whole blood is
7 processed in about 30 mins. The CTC counts obtained from both biochips where they were
8 used for analysis of samples from lung cancer patients is shown in Figure 3C. The
9 multiplexed spiral biochip yielded significant improved capture efficiency in comparison
10 with the previous integrated biochip which processed whole blood. This is also done under
11 shorter time (7.5 mL of blood in 10 mins), giving rise to much higher throughput (Fig. 3D).
12 In addition, the purity of retrieved CTCs captured among contaminating WBCs was
13 significantly higher for the multiplexed biochip, compared with the integrated one.
14
15
16
17
18
19
20
21
22
23
24
25
26
27

28 **Isolation efficiency and cell viability using cancer cell lines**

29 To test the performance of the multiplexed spiral biochip for CTC isolation and recovery, we
30 characterized the biochip with commercially available cancer cell lines. Cell lines have been
31 shown to be a good surrogate for characterization of various microfluidics as well as other
32 CTC enrichment assays. Using the spiral biochip, we demonstrated high recovery of breast
33 (MCF-7) and bladder (T24) cancer cells spiked into healthy blood samples. These cell lines
34 were chosen due to their different range of cell diameters (MCF-7: $\sim 20\ \mu\text{m}$; T24: $\sim 30\ \mu\text{m}$),
35 which validated the ability of the multiplexed spiral biochip for enriching CTCs of different
36 sizes from various cancer types. Following enrichment, cancer cells were identified by
37 immunofluorescence staining either by enumerating under epi-fluorescence microscope or by
38 flow cytometry analysis with common biomarkers (CK+/CD45-). For both cell lines spiked
39 at clinically relevant concentrations of 500/7.5 mL of whole blood, a recovery of 87.6% for
40 MCF-7 and 76.4% for T24 cells was achieved (Fig. 4A).
41
42
43
44
45
46
47
48
49
50
51
52
53
54
55
56
57
58
59
60

1
2
3 To verify cell viability, propidium iodide (PI) staining of recovered samples was performed.
4
5 High viability was confirmed by the minimal staining (<10%) detected by flow cytometry
6
7 (Fig. 4B). Viable cells isolated can then be seeded onto 2-D culture substrates, where they
8
9 attach and proliferate under standard culture conditions. Morphology of cells remained
10
11 relatively unchanged at different stages of processing (before lysis, after lysis and after
12
13 processing with lysis (see Fig. 4C). Isolated cells after device processing also remain viable
14
15 for days after seeding onto culture substrates (See supplementary Fig. 1). This illustrates that
16
17 both the lysis process and shear force induced by device processing did not affect cell
18
19 viability, and is in good agreement with previous studies showing that the high shear
20
21 conditions inside spiral microchannels have no adverse effects on the enriched cells.³¹
22
23
24
25
26

27 **Enrichment of CTCs from patients with metastatic breast and lung cancer**

28
29 Using the optimal test parameters, 7.5 mL of blood samples from 5 healthy volunteers
30
31 (control) and 5 patients with metastatic breast cancer and 5 patients with non-small cell lung
32
33 cancer (NSCLC) were processed (Table 1). CTCs captured by the spiral biochip were
34
35 identified using a comprehensive image analysis algorithm, consisting of staining with
36
37 Hoechst for DNA content, FITC conjugated pan-cytokeratin antibodies for cancer/epithelial
38
39 cells, and APC conjugated anti-CD45 antibodies for haematologic cells (Fig. 5B). Cells
40
41 stained positive for both Hoechst and pan-cytokeratin while negative for CD45 were scored
42
43 as CTCs. CTCs were detected in 10 of 10 patient samples (100% detection) with counts
44
45 ranging from 20-67 CTCs/mL for breast cancer samples and 33-135 CTCs/mL for lung
46
47 cancer samples (Fig. 5A). CTC diameter ranges from 15-25 μm for lung cancer samples and
48
49 20-35 μm for breast cancer samples (data not shown). Epithelial cells positive for pan-
50
51 cytokeratin were also detected in healthy volunteers (1-4 per mL), indicating a clear detection
52
53 threshold.
54
55
56
57
58
59
60

1
2
3 To assess the feasibility of characterizing gene copy number alteration by FISH of CTCs
4 isolated using the multiplexed spiral biochip, we have selected few HER2-positive breast
5 cancer samples for analysis. These samples were obtained from patients with HER2-positive
6 tumor status. HER2-positive breast cancers has been reported to be more aggressive than
7 other types of breast cancer,^{32, 33} however, treatments that specifically target HER2 are very
8 effective.³⁴ HER2 signals in isolated CTCs were compared against control breast cancer cell
9 lines SKBR3 (amplified HER2 signals) and MDA-MB-231 (non-amplified HER2 signal) as
10 shown in Figure 5C. Intriguingly, we found that HER2 status on isolated CTCs did not
11 correlate with primary tumor characteristics. For 3 (out of 5) patients that were analyzed in
12 this study, HER2 status was negative (where amplified HER2 expression was determined
13 when the ratio of HER2/centromere of Chromosome 17 (Cen17) signals in single nuclei was
14 > 2), indicating heterogeneity of HER2 status in disseminated cells and primary tumor.
15
16
17
18
19
20
21
22
23
24
25
26
27
28
29
30
31

32 **Pleomorphism and heterogeneity of enriched CK+ cells**

33
34 Collected CTCs demonstrated intrapatient pleomorphism. Complementing
35 immunofluorescence staining with epifluorescence microscopy detection, we observed
36 differences in cell and nuclear morphology, nuclear-to-cytoplasmic (N/C) ratios and staining
37 pattern. Stained CTCs isolated from the spiral biochip revealed distinct pleomorphic cell
38 types, as shown from the images of CTC provided (Fig. 6A). The CTC varied from cells
39 densely stained at the nucleus and showed eccentric nuclear morphology, to those which had
40 bi-lobed or even kidney shaped nucleus. Such variation in nuclear morphology has also been
41 previously reported³⁵. CTC size also differs with diverse N/C ratios. In some samples, CTC
42 microembolis (clusters) were also observed. In order to further characterise these cells, CTCs
43 were stained for CD166 and CD133, identifying a rare subpopulation (~1 in 135 cells) (Fig.
44
45
46
47
48
49
50
51
52
53
54
55
56
57
58
59
60

1
2
3 6B). CD166 and CD133 are putative cancer stem cell biomarkers that have been associated
4 with tumor progression, poor patient survival and early tumor relapse.^{36, 37}
5
6
7
8
9

10 **Discussion**

11
12 Despite the recent technological advances, development of a simple and robust platform
13 capable of enriching CTCs with high throughput (i.e., processing clinically relevant blood
14 volumes in few mins), high sensitivity, high specificity, and high cell viability remain
15 elusive. The application of microfluidic systems for separation of CTCs provides
16 unprecedented opportunities for efficient enrichments of these rare cells from blood, allowing
17 detailed molecular characterization of them at the single-cell level. Previously, we developed
18 a spiral microfluidic biochip for blood fractionation and applied it successfully for size-based
19 CTCs isolation from blood.²⁶ The integrated biochip developed is capable of processing
20 blood with high hematocrit (~20-25%), thus allowing process and enrichment of tumor cells
21 at ~ 3 mL/hr speed. However, a reduction in processing time will help translate our previous
22 platform to clinic and “point-of-care” applications. Here, we demonstrate the application of a
23 multiplexed spiral biochip for ultra-high throughput isolation of CTCs from lysed blood using
24 inertial focusing microfluidics to realize a single step label-free enrichment process. This
25 device is capable of efficient cell separation of clinically relevant blood volumes in a short
26 period of time (7.5 mL blood in 10 mins), thus allows isolation of viable CTCs with high
27 sensitivity and purity. Compared with other microfluidics-based methods, this device has the
28 following merits. (i) *High throughput processing*: By stacking up a number of biochips, we
29 can further increase the throughput based on the sample volume and downstream assays. (ii)
30 *Simplicity and ease of operation*: the simple design of spiral biochip with large channel
31 dimensions prevent any clogging and facilitate multiplexing and automation for quick
32 translation for diagnostic/prognostic purposes. The simplicity in manufacturing (i.e., no
33
34
35
36
37
38
39
40
41
42
43
44
45
46
47
48
49
50
51
52
53
54
55
56
57
58
59
60

1
2
3 pretreatment or antibody immobilization required) of the device and its ease of operation
4
5 make it attractive for clinical applications requiring one-time use operation. The multiplexed
6
7 spiral biochip demonstrates high sensitivity by the successful detection and isolation of CTCs
8
9 from 100% (10/10) blood samples collected from patients with advanced stage metastatic
10
11 breast and lung cancer. The device also demonstrates high specificity and consistency,
12
13 showing a further improvement and yield over our previous integrated biochip.²⁶ (iii) *Viable*
14
15 *CTC collection*: Unlike affinity-based, electrical or physical filtration platforms, the incessant
16
17 collection of enriched CTCs and short residence time in the micro-channels (<10 msec)
18
19 eliminates the long-shear exposure to the CTCs, hence minimizing any undesirable
20
21 phenotype changes due to the shear stress. The enriched cells are continuously collected in a
22
23 separate tube in real time and can be used for high-definition imaging as well as RNA-based
24
25 single-cell molecular analysis. (iv) *Affordability*: our device uses simple microfluidic
26
27 channels, which can be produced at low-cost using conventional microfabrication techniques.
28
29 In addition, it only needs two plastic syringes for sheath and sample loading into the biochip.
30
31 Further improvement will come in the form of an automated system capable of blood
32
33 handling and processing. Moreover, a critical advantage of this biochip is the ability to return
34
35 all fractions of blood – plasma, CTCs and PBMC – that can be utilized for other diverse
36
37 biomarker studies.
38
39
40
41
42
43
44

45 **Conclusions**

46
47 We demonstrated high-throughput and high-resolution separation of CTCs from blood using
48
49 a multiplexed spiral microfluidic device. This approach utilizes the combined effect of
50
51 inertial and Dean drag force to separate rare cells from large volume of blood samples rapidly
52
53 and efficiently. The label-free nature of the spiral biochip has improved the yield of CTC
54
55
56
57
58
59
60

capture in certain diseases like lung cancer, and current research is directed at cultivating viable CTCs as well as the scalability of detecting clinically actionable genetic alterations.

Acknowledgements

We would like to express our sincere gratitude to all patients who participated in this trial and the healthy volunteers who donated blood samples for characterization of our device. Financial support by the Singapore-MIT Alliance for Research and Technology (SMART) Centre (BioSyM IRG) is gratefully acknowledged. This work is also supported by the use of NTU's Micro-Machine Center (MMC) facilities for wafer fabrication and the lab facilities at the Mechanobiology Institute (MBI) and the Nano Biomechanics Laboratory at the National University of Singapore. The clinical samples and data collection was supported by the Singapore National Medical Research Council grant NMRC 1225/2009.

REFERENCES

1. K. Pantel, R. H. Brakenhoff and B. Brandt, *Nature Reviews Cancer*, 2008, **8**, 329-340.
2. D. R. Parkinson, N. Dracopoli, B. G. Petty, C. Compton, M. Cristofanilli, A. Deisseroth, D. F. Hayes, G. Kapke, P. Kumar and J. S. H. Lee, *Journal of Translational Medicine*, 2012, **10**, 138.
3. M. Yu, S. Stott, M. Toner, S. Maheswaran and D. A. Haber, *The Journal of Cell Biology*, 2011, **192**, 373-382.
4. Y. F. Sun, X. R. Yang, J. Zhou, S. J. Qiu, J. Fan and Y. Xu, *Journal of cancer research and clinical oncology*, 2011, **137**, 1-23.
5. W. He, H. Wang, L. C. Hartmann, J. X. Cheng and P. S. Low, *Proceedings of the National Academy of Sciences*, 2007, **104**, 11760.
6. R. Gertler, R. Rosenberg, K. Fuehrer, M. Dahm, H. Nekarda and J. Siewert, *Recent Results in Cancer Research*, 2003, **162**, 149-156.
7. A. L. Allan, S. A. Vantingham, A. B. Tuck, A. F. Chambers, I. H. Chin-Yee and M. Keeney, *Cytometry Part A*, 2005, **65**, 4-14.
8. I. Cruz, J. J. Cruz, M. Ramos, A. Gómez-Alonso, J. C. Adansa, C. Rodríguez and A. Orfao, *American journal of clinical pathology*, 2005, **123**, 66-74.
9. B. Khoo, M. Warkiani, G. Guan, D. S.-W. Tan, A. S. Lim, W.-T. Lim, Y. S. Yap, S. C. Lee, R. A. Soo and J. Han, Ultra-High Throughput Enrichment of Viable Circulating Tumor Cells, *The 15th International Conference on Biomedical Engineering*, 2014, 1-4.

10. S. Nagrath, L. V. Sequist, S. Maheswaran, D. W. Bell, D. Irimia, L. Ulkus, M. R. Smith, E. L. Kwak, S. Digumarthy, A. Muzikansky, P. Ryan, U. J. Balis, R. G. Tompkins, D. A. Haber and M. Toner, *Nature*, 2007, **450**, 1235-1239.
11. S. L. Stott, C. H. Hsu, D. I. Tsukrov, M. Yu, D. T. Miyamoto, B. A. Waltman, S. M. Rothenberg, A. M. Shah, M. E. Smas and G. K. Korir, *Proceedings of the National Academy of Sciences*, 2010, **107**, 18392-18397.
12. S. Mittal, I. Y. Wong, W. M. Deen and M. Toner, *Biophysical journal*, 2012, **102**, 721-730.
13. C. Alix-Panabières, H. Schwarzenbach and K. Pantel, *Annual Review of Medicine*, 2012, **63**, 199-215.
14. V. Gupta, I. Jafferji, M. Garza, V. O. Melnikova, D. K. Hasegawa, R. Pethig and D. W. Davis, *Biomicrofluidics*, 2012, **6**, 024133.
15. E. Ozkumur, A. M. Shah, J. C. Ciciliano, B. L. Emmink, D. T. Miyamoto, E. Brachtel, M. Yu, P.-i. Chen, B. Morgan and J. Trautwein, *Science translational medicine*, 2013, **5**, 179ra147.
16. H. S. Moon, K. Kwon, S. I. Kim, H. Han, J. Sohn, S. Lee and H. I. Jung, *Lab on a Chip*, 2011, **11**, 1118-1125.
17. E. W. Majid and C. T. Lim, in *Materiomics: Multiscale Mechanics of Biological Materials and Structures*, Springer, 2013, pp. 107-119.
18. J. Chen, J. Li and Y. Sun, *Lab Chip*, 2012, **12**, 1753-1767.
19. S. A. Vona G, Louha M, Sitruk V, Romana S, Schütze K, Capron F, Franco D, Pazzagli M, Vekemans M, Lacour B, Bréchet C, Paterlini-Bréchet P, *Am J Pathol.*, 2000, **156**, 57-63.
20. Z. S. Lin HK, Williams AJ, Balic M, Groshen S, Scher HI, Fleisher M, Stadler W, Datar RH, Tai YC, Cote RJ., *Clinical Cancer Research*, 2010, **16**, 5011-5018.
21. E. J. Lee TK, Blackburn LD, Silverman JF., *Anal Quant Cytol Histol.*, 1992, **14**, 32-34.
22. S. J. Tan, L. Yobas, G. Y. H. Lee, C. N. Ong and C. T. Lim, *Biomedical microdevices*, 2009, **11**, 883-892.
23. M. E. Warkiani, C.-P. Lou and H.-Q. Gong, *Biomicrofluidics*, 2011, **5**, 036504.
24. A. A. S. Bhagat, H. Bow, H. W. Hou, S. J. Tan, J. Han and C. T. Lim, *Medical and Biological Engineering and Computing*, 2010, **48**, 999-1014.
25. E. W. Majid, G. Guan, B. L. Khoo, W. C. Lee, A. A. S. Bhagat, D. S.-W. Tan, W. T. Lim, S. C. Lee, P. C. Chen and C. T. Lim, *Lab Chip*, 2014, **14**, 128-137.
26. H. W. Hou, M. E. Warkiani, B. L. Khoo, Z. R. Li, R. A. Soo, D. S.-W. Tan, W.-T. Lim, J. Han, A. A. S. Bhagat and C. T. Lim, *Scientific Reports*, 2013, **3**:1259.
27. Y. Xia and G. M. Whitesides, *Annual review of materials science*, 1998, **28**, 153-184.
28. M. E. Warkiani, A. A. S. Bhagat, B. L. Khoo, J. Han, C. T. Lim, H. Q. Gong and A. G. Fane, *ACS nano*, 2013, **7**, 1882-1904.
29. A. A. S. Bhagat, S. S. Kuntaegowdanahalli and I. Papautsky, *Lab on a Chip*, 2008, **8**, 1906-1914.
30. S. K. Arya, B. Lim and A. R. A. Rahman, *Lab Chip*, 2013, **13**, 1995-2027.
31. W. C. Lee, A. A. S. Bhagat, S. Huang, K. J. Van Vliet, J. Han and C. T. Lim, *Lab on a Chip*, 2011, **11**, 1359-1367.
32. C. G. Slamon DJ, Wong SG, Levin WJ, Ullrich A, McGuire WL., *Science*, 1987, **235**, 177-182.
33. G. W. Slamon DJ, Jones LA, Holt JA, Wong SG, Keith DE, Levin WJ, Stuart SG, Udove J, Ullrich A, Michael FP, *Science*, 1989 **244**, 707-712.
34. S. Riethdorf, V. Müller, L. Zhang, T. Rau, S. Loibl, M. Komor, M. Roller, J. Huober, T. Fehm and I. Schrader, *Clinical Cancer Research*, 2010, **16**, 2634-2645.

- 1
2
3 35. D. Marrinucci, K. Bethel, D. Lazar, J. Fisher, E. Huynh, P. Clark, R. Bruce, J. Nieva
4 and P. Kuhn, *Journal of oncology*, 2010, **2010**, 1-7.
5 36. C. Kahlert, H. Weber, C. Mogler, F. Bergmann, P. Schirmacher, H. Kenngott, U.
6 Mattered, N. Mollberg, N. Rahbari and U. Hinz, *British journal of cancer*, 2009, **101**,
7 457-464.
8 37. A. Lugli, G. Iezzi, I. Hostettler, M. Muraro, V. Mele, L. Tornillo, V. Carafa, G.
9 Spagnoli, L. Terracciano and I. Zlobec, *British journal of cancer*, 2010, **103**, 382-390.
10
11
12
13

14 Table Captions:

15 **Table 1.** Clinico-pathological characteristics of patients enrolled in this study for CTC enumeration
16 (C: Cycle, D: Day, Sutent: Sunitinib).
17

18
19
20 Figure Captions:

21
22 **Figure 1.** (A) Schematic representation of the configuration and operational mechanism of a
23 multiplexed spiral microfluidic chip for capturing CTCs with two inlets and two outlets. (B) Sample
24 processing workflow showing different steps of enrichment and identification. The blood sample is
25 collected; RBCs are lysed and processed through multiplexed spiral biochip. The isolated CTCs are
26 available for immunostaining using specific markers or FISH. DNA or RNA can be extracted from
27 the CTCs and subjected to next-generation sequencing and quantitative RT-PCR (qRT-PCR). Viable
28 cells can be released and propagated in cell culture for various applications including cancer stem cell
29 (CSC) study or drug discovery.
30

31 **Figure 2.** (A) Time sequence images demonstrating the isolation of rare cells using the spiral
32 microfluidic biochip. Using advantage of the inherent secondary Dean vortex flows present in
33 curvilinear microchannels, the CTCs (marked with black arrow) can be focused near the microchannel
34 inner wall while driving the smaller hematologic cells (RBCs and WBCs) toward the microchannel
35 outer wall, thus allowing an efficient separation at the outlet. Scale bar is 100 μm . (B) Different WBC
36 concentration affects the total number of nucleated cells collected at the first 5 mins of processing
37 ($n=3$; Anova (single factor), $P<0.05$). (C) Linear increase in nucleated cells isolated along with the
38 respective increase in whole blood processed under 2x concentration. This demonstrates the relatively
39 constant rate of nucleated cell collection with time. ($n=3$; Anova (single factor), $P<0.05$).
40

41 **Figure 3:** (A) Minimal cell loss incurred upon cell lysis. Flow cytometry quantification for recovery
42 of spiked T24 cells is comparable to that enumerated for recovery of cells spiked in whole blood (98%
43 with respect to recovery in whole blood) ($n=3$; Anova, $P= 0.82$). (B) Range of MCF-7 cell diameters
44 after exposure to different media. No significant increase in cell diameter is detected ($n=3$; Anova, $P=$
45 0.2). (C) CTC count obtained by the integrated spiral biochip is compared against that of the current
46 multiplexed spiral using blood of patients with lung cancer. (D) Sample processing time by the
47 integrated spiral biochip was compared with that of the current multiplexed spiral biochip (i.e., for 7.5
48 mL of blood).
49

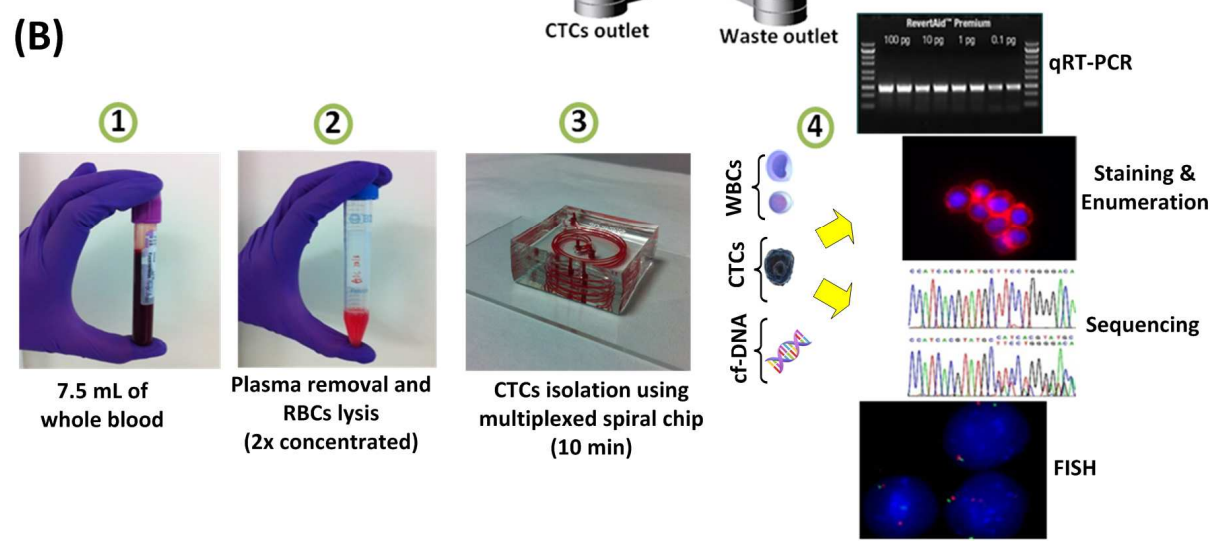
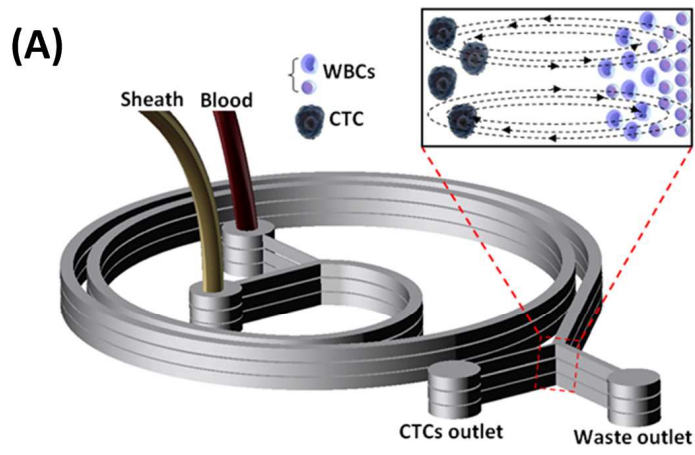
50 **Figure 4.** (A) Recovery of spiked cancer cells introduced at clinically relevant concentration (500
51 cells per 7.5 mL whole blood) ($n=3$; Anova (single factor), $P<0.05$). (B) Proportion of viable cells
52 after various treatments, as stained by propidium iodide (B.P: Before Processing & A.P: After
53 Processing). (C) Phase contrast microscopy images of isolated T24 at different treatment conditions.
54 Morphology of cells remained relatively constant after lysis and spiral processing treatments, and
55 cells remained viable. Cancer cells are indicated by orange arrows. Scale bar is 10 μm .
56
57
58
59
60

Figure 5. Enumeration of CTCs from cancer patients. (A) Plot of CTCs enumeration for healthy donors (Red), breast cancer patients (Black) and lung cancer patients (Blue). (B) Immunofluorescence staining of isolated CTCs. CTCs (marked by white arrow) were identified by the following criteria: Hoechst positive, pan-cytokeratin positive and CD45 negative. Scale bar is 16 μm . (C) FISH for HER2 detection for breast cancer cell line MDA-MB-231, SKBR3 and breast CTC enriched by the multiplexed spiral chip. Nuclei of cells were stained with DAPI, HER-2/neu gene locus (red) and CEP 17 centromere (green). Scale bar is 10 μm .

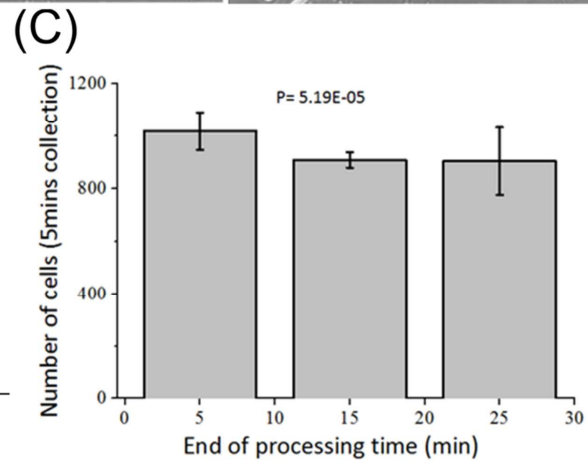
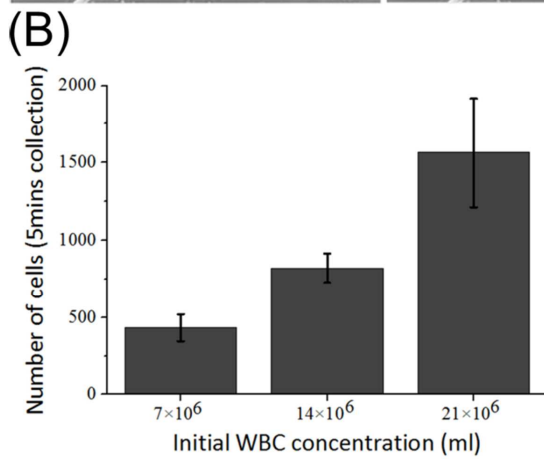
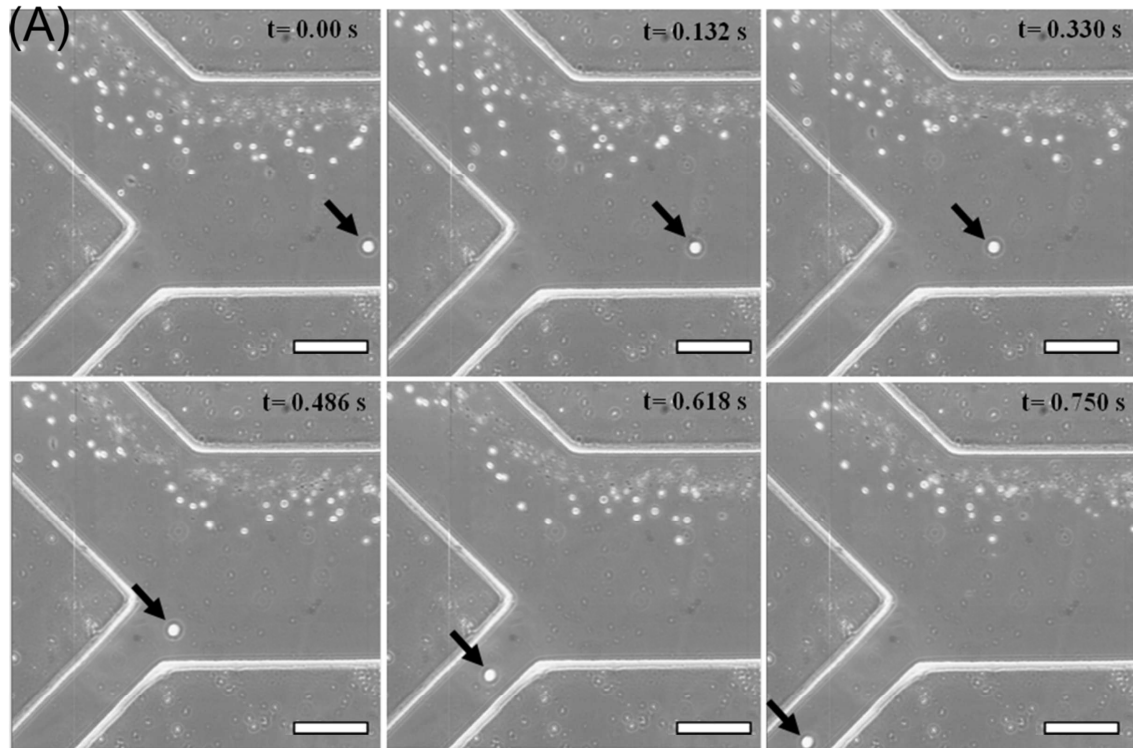
Figure 6. (A) CTC nuclear and cell size pleomorphism. Isolated CTCs displayed varied range of nuclear shapes and cell size (Blue: Hoechst & Green: CK). (B) Staining for stem cell markers on lung CTCs. Population of CD166+ cells were rare in most of the samples. In some occasions, some CD166+/CD133+ cells were also detected in certain samples. Scale bar is 10 μm .

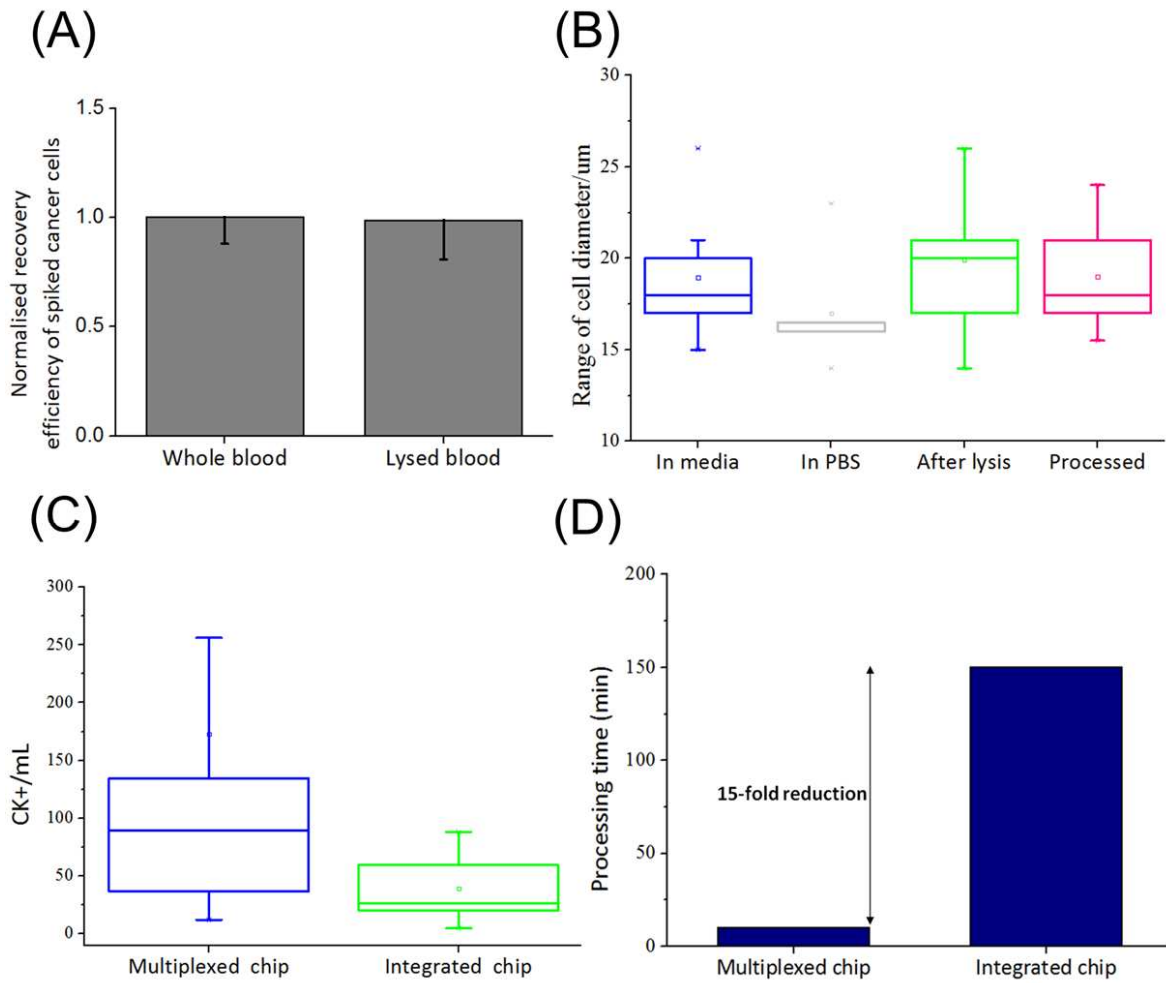
Sample no	Subject status	CK+ cells/mL	Cancer stage	Treatment timepoint
1	Healthy	1	N.A.	N.A.
2	Healthy	3	N.A.	N.A.
3	Healthy	3	N.A.	N.A.
4	Healthy	4	N.A.	N.A.
5	Healthy	2	N.A.	N.A.
1	Breast	20	IV	C1D15
2	Breast	61	IV	Post Sutent
3	Breast	55	IV	C1D15
4	Breast	34	IV	Baseline
5	Breast	67		Baseline
1	Lung	33	IV	Single Draw
2	Lung	43	IV	Single Draw
3	Lung	37	IV	Single Draw
4	Lung	90	IV	Single Draw
5	Lung	135	IV	Single Draw

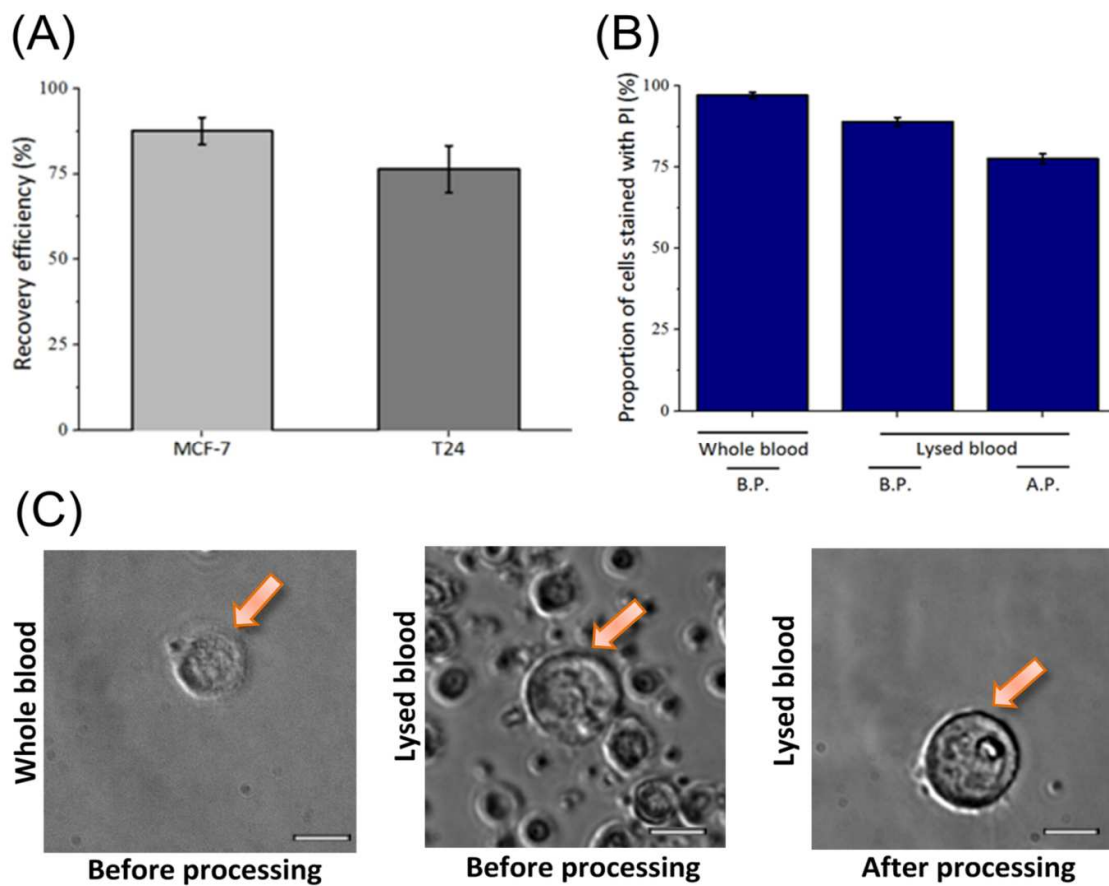
1
2
3
4
5
6
7
8
9
10
11
12
13
14
15
16
17
18
19
20
21
22
23
24
25
26
27
28
29
30
31
32
33
34
35
36
37
38
39
40
41
42
43
44
45
46
47
48
49
50
51
52
53
54
55
56
57
58
59
60



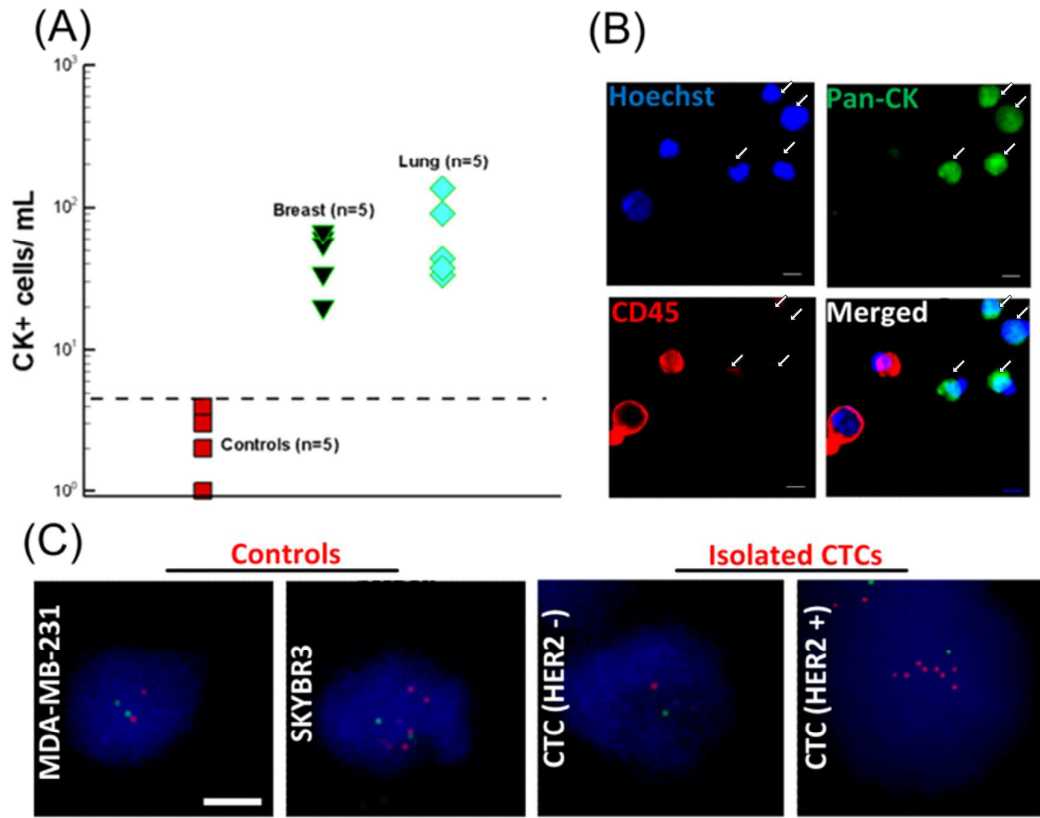
Analyst Accepted Manuscript







1
2
3
4
5
6
7
8
9
10
11
12
13
14
15
16
17
18
19
20
21
22
23
24
25
26
27
28
29
30
31
32
33
34
35
36
37
38
39
40
41
42
43
44
45
46
47
48
49
50
51
52
53
54
55
56
57
58
59
60



Analyst Accepted Manuscript

